表1 神経芽腫の予後因子

	予後	
	良好	不良
年齢	1歳未満	1歳以上
病期 (INSS)*	1, 2, 4S	3, 4
組織型 (Shimada分類)	favorable histology	unfavorable histology
MYCN の増幅	なし	あり
DNA ploidy	Aneuploid (hyperdiploid)	Diploid Tetraploid
1p欠失またはLOH	なし	あり
17q gain	なし	あり
TRK-A の発現	あり	なし
血中フェリチン	< 142 ng/mL	> 142 ng/mL
血中NSE	< 100 ng/mL	> 100 ng/mL

* INSS: International Neuroblastoma Staging System

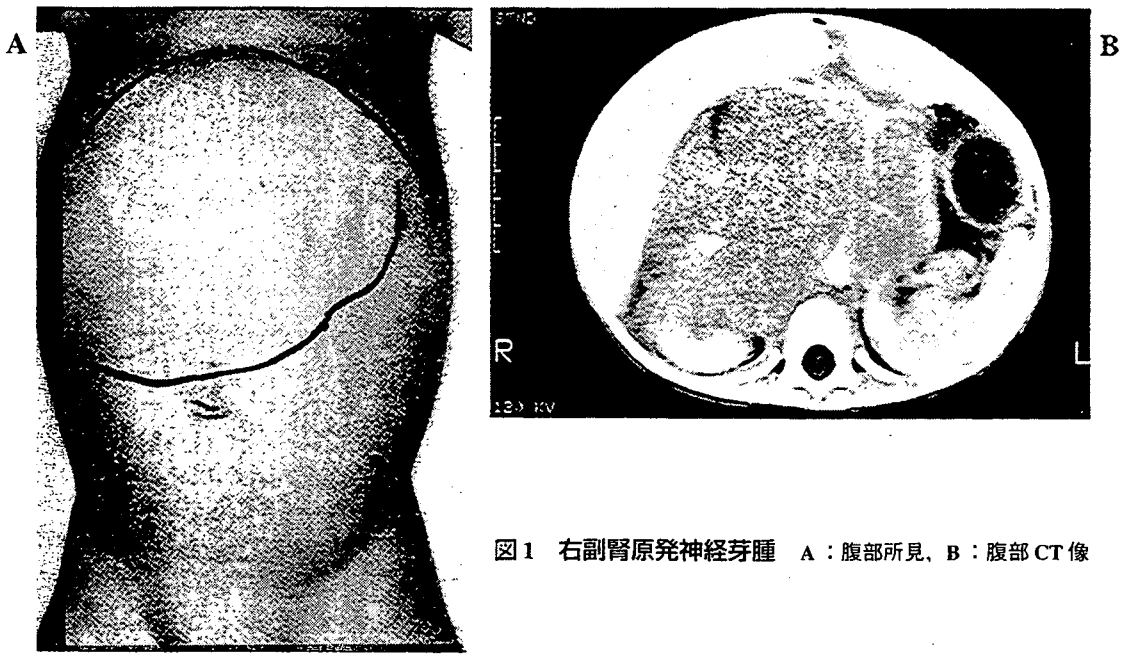

図1 右副腎原発神経芽腫 A：腹部所見、B：腹部CT像

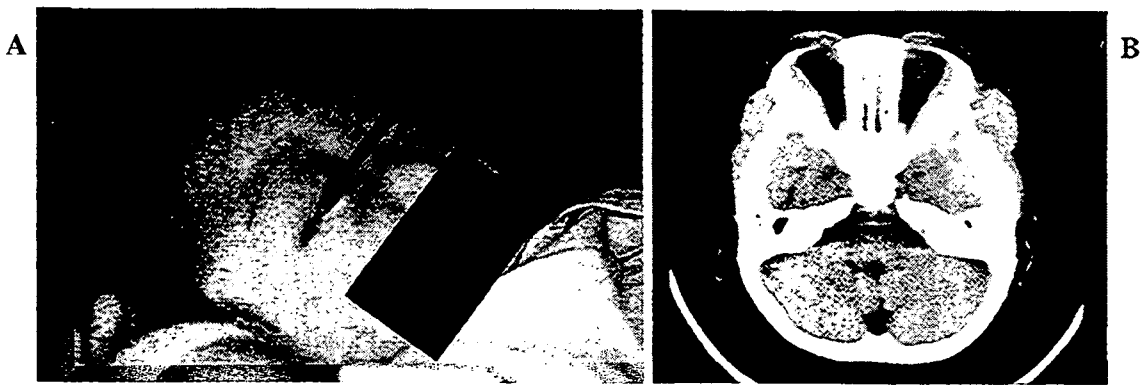

図2 神経芽腫の眼窩転移
A：両側眼球の突出と眼周囲の出血斑．B：頭部CTでは眼窩周囲の骨破壊と腫瘤像を認める

できる症例も多く認められる.

このほか，Shimada分類に基づく組織型，がん遺伝子*MYCN*増幅の有無，DNA diploidyなどが生物学的悪性度を反映する重要な予後因子であり，わが国では一般に，年齢，病期，*MYCN*増幅の有無などにより悪性度を判定し，治療の選択を行っている.

治療成績は1歳未満の神経芽腫では大多数の例で悪性度は低く，摘出術±化学療法で95%を超える5年生存率が得られている[1].

したがって，治療は腫瘍の圧迫による呼吸障害や，肝・腎などの臓器障害の回避を優先する.抗腫瘍療法は最小限で奏効することが多く，とくに，臓器や大血管の合併切除を行うような手術は厳に慎むべきである.ただし乳児期の神経芽腫でも，骨や遠隔リンパ節への転移を伴う症例や2～3%の*MYCN*増幅例では，進行神経芽腫に準じた強力な治療が必要となる.

表2 神経芽腫の治療成績

年齢	病期 (INSS)	5年生存率
＜1歳	1, 2, 3, 4S	95%以上
	4	70%
	any stage, *MYCN*増幅あり	40%
＞1歳	1, 2	95%以上
	3	75%
	4	30%

一方，1歳以上の進行症例の治療成績は依然，5年生存率で30%を上回る程度である（表2）[1].1歳以降では，診断時にすでに腫瘍が切除不能と判断される症例や，骨，リンパ節に遠隔転移を認める症例が75%を超え，*MYCN*増幅例も30%に認められる.これらの腫瘍では手術，化学療法，放射線療法，造血幹細胞移植などを組み合せた積極的な治療が行われるが，上記のように，治療成績はいまだ不良であり，有効な新規治療法の開発が待たれている.

腎芽腫（Wilms腫瘍）

腎芽腫は小児期の代表的な悪性腎腫瘍で，胎生期の後腎芽細胞（metanephrogenic blastema）から発生すると考えられている.米国では，年間500人の新たな患者の発生があり，100万人に7.9人の頻度で小児腫瘍の6.3%を占めるとされるが[2]，わが国の年間登録数は数十例程度である.腎芽腫の75%は3歳までに発症し，同時性両側性の症例が5%の頻度で，また家族内発生例も1%に認められる.無症状の腹部腫瘤として発見される場合が多いが，血尿や腫瘍破裂に伴う腹痛などを主訴に診断されることもある（図3）.

腎芽腫には5～12%の頻度で無虹彩症，片側肥大，停留精巣，尿道下裂などの先天奇形を合

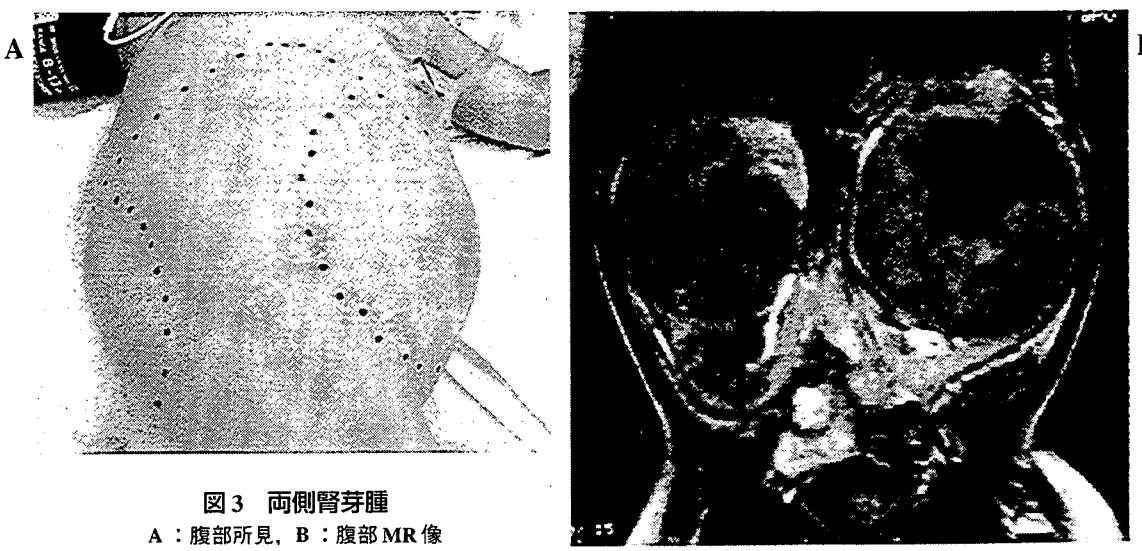

図3 両側腎芽腫
A：腹部所見，B：腹部MR像

併する（**表3**）．とくに腎芽腫に無虹彩，泌尿生殖器奇形，精神発達遅延を合併したものをWAGR症候群，腎疾患，生殖器奇形を合併したものをDenys-Drash症候群という．

一方，身体の一部の過成長や肥大を伴う症候群と腎芽腫との関連も知られており，Beckwith-Wiedemann症候群では腎芽腫のほか，肝芽腫，横紋筋肉腫，副腎皮質腫瘍などの発生をみることがある．

WAGR症候群では，11番染色体短腕13領域（11p13）に欠失のあることが知られていたが，1990年，11p13に位置するがん抑制遺伝子WT-1が単離された[3]．WT-1は，腎および泌尿生殖器の分化に関連する転写調節因子で，WAGR症候群のほか，Denys-Drash症候群および一部の腎芽腫の原因遺伝子と考えられている．一方，Beckwith-Wiedemann症候群にみられる染色体異常は11p15.5の異常であり，この部位に，第二の腎芽腫原因遺伝子WT-2の存在が想定されている．WT-2の有力な候補である*IGF2*遺伝子は，一部の腎芽腫で過剰発現が観察されており，その過剰発現が臓器の過成長や肥大，また腎芽腫の発生原因になると考えられている．

腎芽腫の前がん病変と考えられているnephrogenic rests，あるいは腎芽腫症（nephroblastomatosis）は，正常腎組織内における後腎芽細胞の遺残で，腎芽腫の30～40%に認められ，新生児の剖検例でも1%の頻度で観察される．この病変は，腎内の存在部位によりintralobar nephrogenic rests（ILNR）とperilobar nephrogenic rests（PLNR）に分類される．

わが国における腎芽腫の治療は，一般に米国のグループ研究National Wilms Tumor Study（NWTS）の治療プロトコールに従って行われることが多い．すなわち組織型がfavorable histologyで病期がⅠ，Ⅱであれば，腫瘍摘出後にactinomycin D（AMD）とvincristine（VCR）による化学療法を行う．一方，Ⅲ，Ⅳでは腫瘍摘出後にAMD，VCR，adriamycin（ADR）の3剤併用療法と放射線療法を行う．さらに，病期Ⅴの同時性両側性の腎芽腫では，腎機能を可及的に温存する治療戦略が選択される．現在，腎芽腫全体の生存率は90%を超えるともいわれており[4]，晩期障害を回避すべく，縮小治療の開発研究が行われている．しかし腎芽腫は，肺や局所に転移再発することもまれでなく，治療終了後も慎重に経過観察する必要がある．

小児肝がん

小児期の原発性肝腫瘍は，小児腫瘍全体の0.5～2%で，良性および悪性の上皮性腫瘍と間葉系腫瘍が含まれる[5]．悪性腫瘍は肝腫瘍全体の55～65%で，その90%が肝芽腫または肝細胞がん（成人型肝がん）である[6]．鑑別すべきその他の腫瘍にはfibrolamellar carcinoma，未分化肉腫，胆道原発の横紋筋肉腫などに加え，卵黄

表3　腎芽腫の先天異常と原因遺伝子

過成長	症候群・症状・前がん病変	原因遺伝子	遺伝子座	遺伝子のはたらき
なし	WAGR症候群 Denys-Drash症候群 intralobar nephrogenic rests（ILNR）	がん抑制遺伝子WT-1	11p13	腎・泌尿生殖器の分化 転写調節
あり	Beckwith-Wiedemann症候群 片側肥大 Perlman症候群 perilobar nephrogenic rests（PLNR）	WT-2？	11p15.5	

表4 小児肝腫瘍の好発年齢

乳幼児期（～5歳）	肝芽腫
	横紋筋肉腫
	乳児血管内皮腫
	間葉性過誤腫
学童期以降（6歳～）	肝細胞がん
	未分化肉腫

嚢腫瘍，絨毛がん，転移性肝腫瘍（神経芽腫など）などがある．

一方，良性腫瘍の大部分は血管腫で，ほかに間葉性過誤腫など小児に特異な腫瘍がある．それぞれの腫瘍には好発年齢があるので，鑑別診断の際には患児の年齢を参考とする（表4）．

1．肝芽腫

肝芽腫の45％は1歳前に，また80％は4歳未満で発症し男児にやや多い[6]．多くは散発例であるが，数％にBeckwith-Wiedemann症候群，片側肥大，家族性大腸ポリポーシス，18トリソミーなどを伴う．また，低出生体重児においても高率に肝芽腫が発生することが知られている[7]．

肝芽腫ではβ-カテニン遺伝子の異常が認められ，腫瘍発生への関与が示唆されている．β-カテニン蛋白は，家族性大腸ポリポーシス症で異常のみられるadenomatous polyposis coli（APC）遺伝子産物により分解されるため，β-カテニンやAPCに異常がある場合，β-カテニンが分解されずに細胞内に蓄積し，β-カテニンの転写活性が亢進し，肝細胞ががん化すると仮説されている．

初発症状は腹部腫瘤，腹痛，発熱などで，食思不振，体重減少，貧血などの症状もみられる．画像検査は腫瘍の性状，局在診断，切除可能性などの評価を目的に腹部超音波検査，CT，MRIなどが行われる．また肺，腹部リンパ節，骨などへの転移の有無を検索する目的でCT，骨シンチが必要である．腹部単純X線検査では石灰化がみられることもある．肝芽腫は通常，肝内の単発性腫瘤として発生するが，20％の症例では，多発性またはびまん性の浸潤形態を示し，転移は肺に多い．組織学的には高分化型（胎児型，fetal type），低分化型（胎芽型，embryonal type），未熟型などに分類され，とくに胎児型の亜型である純高分化型（pure fetal type）の予後は良好である．

肝芽腫では，血中のα-フェトプロテイン（AFP）がほぼ全例で高値を示すため，腫瘍マーカーとして用いられる．性早熟を伴う症例では血中のβ-hCGが高値を示す．血小板増多や高コレステロール血症もしばしばみられ，骨粗鬆症を合併することもある．

治療は外科的切除の役割が大きく，切除の可否が重要な予後因子である．原発巣を一期的または二期的に切除し，同時にcisplatin（CDDP）やTHP-adriamycinなどによる化学療法を行う．原発巣が切除不能な症例や，診断時に遠隔転移を伴う症例では，化学療法を優先し，腫瘍の縮小を待って切除を行う．肺転移巣も化学療法と切除によりコントロールが可能である．腫瘍が肝に限局し，かつ，切除不能な症例に対しては肝移植の適応が検討される．

わが国では，一期的切除が可能な症例では95％以上の生存率が得られ，化学療法が先行される進行例では39～74％の治療成績である[8]．

2．肝細胞がん（成人型肝がん）

肝細胞がん（成人型肝がん）は，小児肝悪性腫瘍の10～30％を占め，肝芽腫に次いで多い．男児に多く，好発年齢は学童期以降である．

肝細胞がんはチロシン血症，胆道閉鎖症，新生児肝炎，α_1-アンチトリプシン欠損症などの慢性肝疾患からも発生する．長期間の中心静脈栄養に起因する肝硬変や，B型肝炎ウイルス感染も肝細胞がんの発生原因である．

初発症状は肝芽腫と同様，腹痛や腹部腫瘤で，発熱，体重減少，黄疸のほか，腫瘍破裂による出血性ショックを呈することもある．血清の

AFPは50～80%の症例で高値を示す．また肝細胞がんでは，satellite lesionや門脈内浸潤の頻度が高いこともその特徴である．

肝細胞がんは化学療法に対する反応性が乏しく，したがって，切除不能例の予後は不良である[9]．完全切除が可能な症例は10～20%程度で，切除不能例では2年以内に死亡する例が多い．

腹部固形腫瘍を見逃さないために

神経芽腫，腎芽腫，肝芽腫などの腹部固形腫瘍は固い腫瘤として触知され，同時に腹部の膨隆を認めることが多い．日頃から胸部の聴打診とともに，丹念に腹部所見をとる習慣を身につけることが，これらの腫瘍に代表される腹部の腫瘤性病変を見逃さないために，きわめて重要である．

また，触診により腹部の固形腫瘍を疑った際には，腹部の超音波検査が第一選択である．超音波検査により腹部腫瘤の存在を確認したら，速やかに腹部の画像診断や腫瘍マーカーの検索を行える施設に，患児を紹介または転送する．これらの施設において，本稿で述べた腫瘍の存在が診断されたら，小児がんの治療のできる施設において治療が行われるべきである．

文　献

1) Ikeda H, Iehara T, Tsuchida Y et al.: Experience with International Neuroblastoma Staging System and Pathology Classification. Br J Cancer 86: 1110-1116, 2002
2) Bernstein L, Linet M, Smith MA et al.: Renal tumors. In: Cancer Incidence and Survival among Children and Adolescents: United States SEER Program 1975-1995. National Cancer Institute Publication, 79-90, 1999
3) Call KM, Glaser T, Ito CY et al.: Isolation and characterization of a zinc finger polypeptide gene at the human chromosome 11 Wilms'tumor locus. Cell 60: 509-520, 1990
4) D'Angio GJ: The National Wilms Tumor Study: A 40 year perspective. Lifetime Data Anal 13: 463-470, 2007
5) Stocker JT, Husain AN, Dehner LP et al.: Hepatic neoplasms. In: Stocker JT, Dehner LP (eds.): Pediatric Pathology (2nd ed.), Lippincott Williams & Wilkins, Philadelphia, 752-795, 2001
6) Ikeda H, Matsunaga T, Tsuchida Y et al.: In: Vöute PA, Barrett A, Stevens MCG, Caron HN (eds.): Cancer in Children (5th ed.), Oxford University Press, Oxford, 370-383, 2005
7) Ikeda H, Matsuyama S, Tanimura M: Association between hepatoblastoma and very low birth weight: A trend or a chance? J Pediatr 130: 557-560, 1997
8) Sasaki F, Matsunaga T, Iwafuchi M et al.: Outcome of hepatoblastoma treated with the JPLT-1 (Japanese Study Group for Pediatric Liver Tumor Protocol-1): A report from the Japanese Study Group for Pediatric Liver Tumor. J Pediatr Surg 37: 851-856, 2002
9) Katzenstein HM, Krailo MD, Malogolowkin MH et al.: Hepatocellular carcinoma in children and adolescents: Results from the Pediatric Oncology Group and the Children's Cancer Group intergroup study. J Clin Oncol 20: 2789-2797, 2002

著者連絡先
〒343-8555　埼玉県越谷市南越谷2-1-50
獨協医科大学越谷病院小児外科
池田　均

■ 特集 小児固形腫瘍の分子生物学（その 3）：最新の知見

肝芽腫の分子生物学

鈴木 信* 池田 均* 小川誠司** 林 泰秀***

はじめに

肝芽腫は，主に 3 歳以下の乳幼児期に好発する胎児性腫瘍の性格を示す肝悪性腫瘍である。化学療法の改良と手術技術の進歩により生存率の改善が認められてはいるが，巨大腫瘍や遠隔転移により未だ予後不良なものも存在する。肝芽腫の発生に関しては低出生体重児[1]，家族性大腸腺腫症(FAP)[2]および Beckwith-Wiedemann 症候群(BWS)[3]との関連が報告されているものの，未だ確定した発生要因は見つかっておらず，その多くは散発性であるのが現状である。

近年，ヒトゲノム情報の充実とその解析を可能とするゲノミクス技術の発達により，腫瘍発生にかかわるさまざまながん関連遺伝子が単離され，それらの不活化が多くの腫瘍の発生・進展に関与することが解明されてきた。がん抑制遺伝子を不活化する主なメカニズムには，ヘテロ接合性の消失（LOH），点突然変異およびメチル化などがある。とくに LOH は多くの腫瘍で特異的な染色体領域が報告されており，それらの領域からいくつかのがん抑制遺伝子が単離されている。肝芽腫においてもがん関連遺伝子に関するさまざまな研究がなされ，そのなかでいくつかの特異的な LOH，変異およびメチル化が報告されているが，疾患遺伝子の同定には至っていない。

本稿では，肝芽腫における遺伝子異常に関し，新たな分子生物学的研究手法による解析の自験例を含め最近の知見を概説する。

* 獨協医科大学越谷病院小児外科
〔〒343-0855 越谷市南越谷 2-1-50〕
** 東京大学大学院 21 世紀 COE プログラム
*** 群馬県立小児医療センター血液腫瘍科

Ⅰ．肝芽腫における染色体・ゲノム異常

肝芽腫における染色体・ゲノム異常は，従来の染色体分染法，FISH，CGH 等の方法による 2，20，1(1q) および 8 番染色体の異常の報告が比較的多くみられ[4]，最も一般的な異常は 2，20 番染色体のトリソミーである。また，1 番染色体の異常は他の腫瘍同様に比較的多く認められる。とくに 1q12-q21 の異常を多く認め，*NTRK1*，*ABL2*，*CD34*，*DAP3* および caspase 3 などが関連遺伝子と考えられている[4]。近年，染色体解析の領域にもマイクロアレイ技術が導入されアレイ CGH などに代表されるように，染色体のコピー数変化を網羅的に解析することが可能となってきた。**図 1** に，われわれがオリゴヌクレオチドマイクロアレイを用いて検討した肝芽腫におけるゲノムコピー数の変化のまとめを示す。少数ながら，われわれの検討でも染色体 1q，2，8，17q，20 番の共通した増加を認め，さらに 7q34，14q11.2 に高頻度な増幅領域を認めた（現在投稿中）。

肝芽腫における LOH に関して 11p15.5[5]および 1p における報告を認める。とくに 11p15 の領域は，BWS 責任遺伝子部位であり肝芽腫の病因にかかわる可能性が示唆されている。前述のわれわれの検討では，17 例中 4 例と比較的高率に 11p15 領域における染色体コピー数の異常を伴わない LOH である uniparental disomy（UPD）を認めた。この UPD は，メチル化の状態の検索より両アレルとも父由来であることがわかり，11p15 領域に存在するインプリンティング遺伝子の機能不全もしくは過剰発現が肝芽腫発生の病態に関与している可能性が示唆された（**図 2**）。

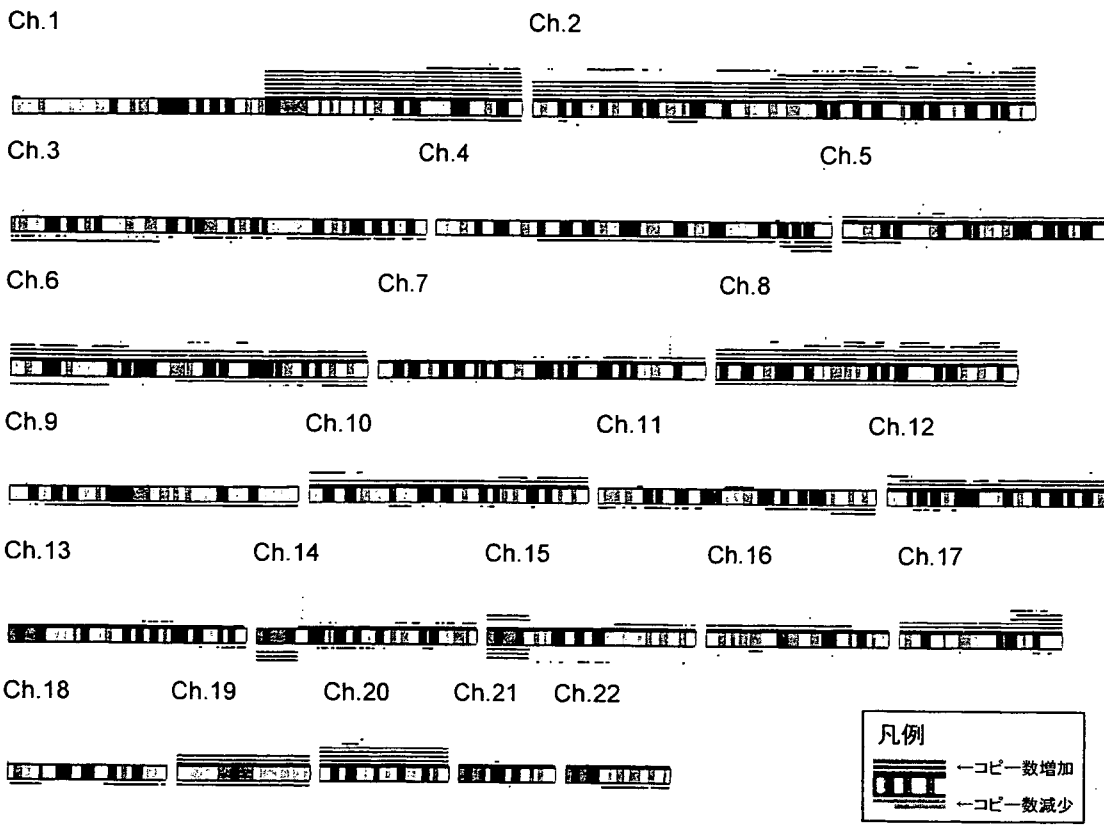

図 1 ゲノムアレイを用いたコピー数の解析

Affymetrix 社 GeneChip®Mapping 50K *XbaI* アレイを用いた 17 例の肝芽腫症例についてのコピー数の増減の解析において 1q, 2(q), 8, 17(q), および 20 番染色体の増加が認められた。

II. 肝芽腫における遺伝子異常

βカテニン遺伝子（*CTNNB1*）はヒト染色体 3q21 に存在し，16 の exon と 15 の intron から構成される。exon 3 が GSK-3β リン酸化部位を含む領域をコードし，同部位での点突然変異や欠失変異が肝芽腫においても高率に認められている[6]。通常βカテニン蛋白は APC 蛋白や Axin 蛋白とともに複合体を形成しリン酸化され分解されるが，これらに変異が生じると分解が阻害されβカテニンの蓄積が進む。蓄積したβカテニンは核へと移行し，ターゲット遺伝子の過剰活性化が進む。免疫染色でもβカテニン蛋白は，正常肝細胞においては細胞膜周辺のみが染色されるのに対し，肝芽腫細胞では核および細胞質が濃染され，蛋白の核内移行・蓄積が認められる[6]。われわれの検討でも，全例にβカテニン蛋白の核内移行を認め，その一部にターゲットとされる cyclinD1 蛋白の集積を確認した（**図 3**）。

肝芽腫の発生には *APC*, *AXIN1*, *AXIN2* の遺伝子異常も同様に関与していると考えられるが，βカテニンを含む Wnt/wingless シグナル伝達経路と組織型・予後との関連は認めないとの報告もあり，さらなる検討が必要である。

その他，8 番染色体の増幅と関連して *IGF2* の制御因子である *PLAG1* の増幅・過剰発現が認められ肝芽腫の発生との関連が報告されている[7]。

III. 肝芽腫におけるエピジェネティクス異常

エピジェネティクスとは，塩基配列の変化以外の染色体修飾による遺伝子発現調節機構のことを指し，具体的にはゲノム DNA のメチル化，ヒストンの修飾（アセチル化，メチル化，リン酸化など），染色体の高次構造変化などを含む。エピジェネティック変化は疾患の薬剤反応性においても重要な役割を果たしていることが知られている。

RASSF1A は 3p21 に存在し，腫瘍増殖やアポトーシスを制御するがん抑制遺伝子のひとつであ

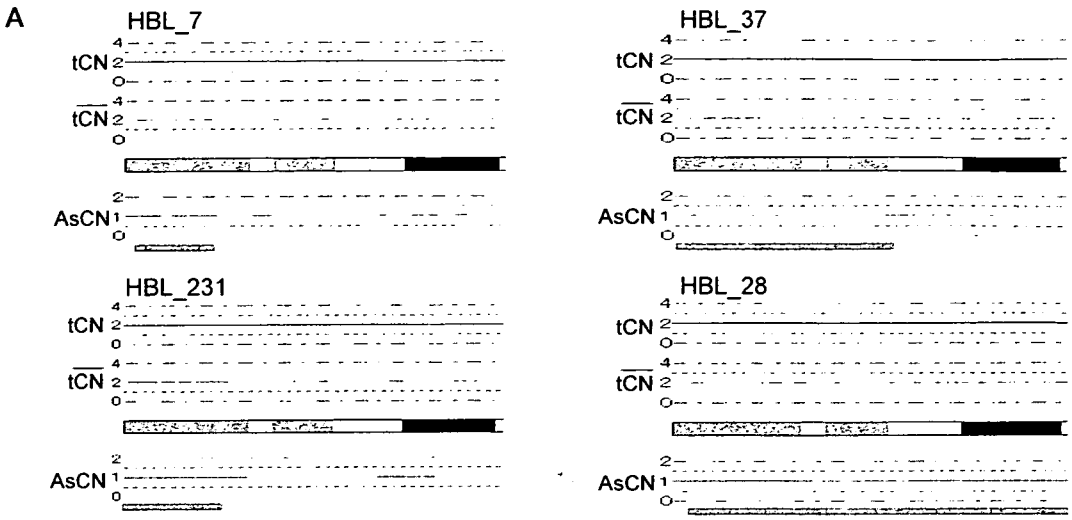

図 2 肝芽腫における 11p15 領域におけるアレル異常

A：11p15 領域に総コピー数の変化を見かけ上伴わない LOH (uniparental disomy) を 17 例中 4 例に認めた。
B：通常では，父方アレルがメチル化，母方アレルが非メチル化されている 11p15 領域に存在する *H19* 遺伝子上流の *H19DMR* 部位でのメチル化解析により，父方アレル由来の UPD であることを確認した。

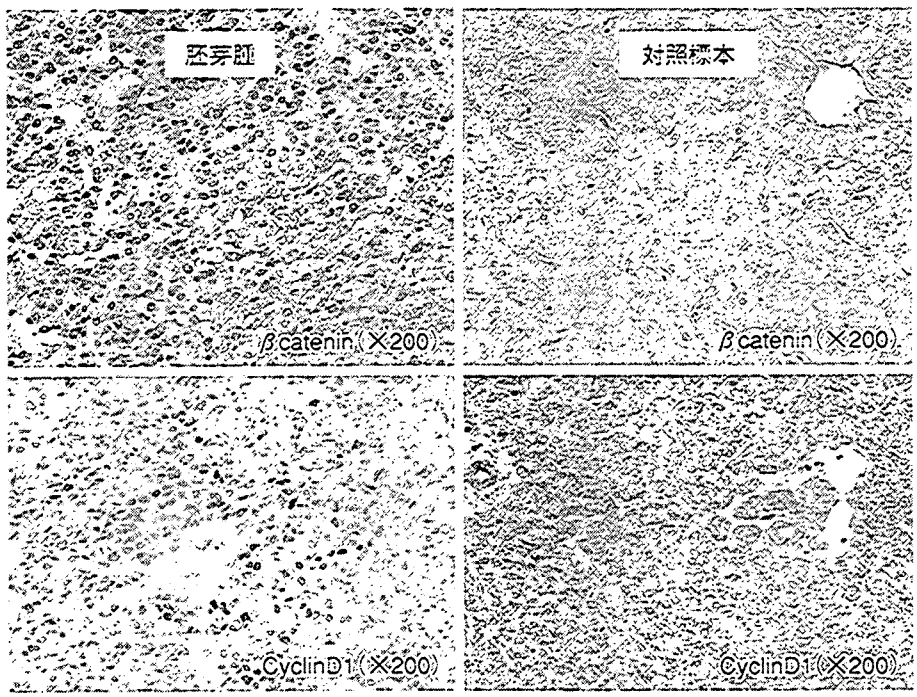

図 3 肝芽腫症例におけるβカテニンおよび cyclinD1 抗体を用いた免疫染色
肝芽腫症例ではβカテニンおよび cyclinD1 ともに核内濃染像を認める。

るが，プロモータ部にメチル化が生じると，その発現が抑制されることがさまざまな腫瘍で認められている。肝芽腫においても同様で，*RASSFA1* のメチル化と予後との関連が報告されている[8]。また，*IGF2* および *H19* 遺伝子においてもメチル化とインプリンティングの消失との関連が報告されている[9]。

IV. マイクロアレイによる網羅的解析

近年，さまざまな疾患発症機構それぞれを特異的に解析するだけでなく，全体の変化を認識・判別する手法として，DNA マイクロアレイによる網羅的発現解析が活用されている。マイクロアレイに関しては前稿および他稿を参照していただきたいが，肝芽腫に関してもさまざまなマイクロアレイ技術を用いた解析が現在行われている。

発現アレイでは，遺伝子発現を網羅的に解析し，クラスター分類することにより，正常対照と比較して肝芽腫における発現が変化している遺伝子につき，組織型や予後等と関連があるだろうと推測できる候補遺伝子を，列挙することが可能である。永田ら[10]は，この手法を用い候補遺伝子として *IGF2* を含む 26 遺伝子を挙げている。

さらにゲノムワイドに全染色体を対象に DNA のコピー数の異常を検出できる方法として，アレイ CGH 法が多く用いられている。アレイ CGH は腫瘍ゲノムと正常ゲノムを同一アレイ上でハイブリダイズし，比較するものでコピー数の異常を伴わない染色体異常（UPD）は検出できなく，正常対象を持たない検体の検索は困難であった。こうした点を補うべくわれわれは，前稿で述べられている SNP 特異的なオリゴヌクレオチドアレイ（Affymetrix 社 GeneChip® Mapping 50K *Xba*I array）および正常対照を持たない検体でもアレルごとのコピー数の解析を可能としたアルゴリズム（CNAG/AsCN）[11,12]を用い，肝芽腫におけるアレルごとのコピー数の変化を網羅的に検索することによってさまざまな LOH，UPD 等の前述のような異常を検索することができた。

最後に，エピジェネティクス解析の領域でも ChIP-on-chip 法をはじめとするさまざまなマイクロアレイ技術を用いた解析法が開発されている。肝芽腫における報告は現在のところ認めないが，こうした高密度なマイクロアレイを用いた解析により，ゲノムワイドなメチル化の検出に加えてヒストンアセチル化の解析などが可能であり，今後，肝芽腫においてもエピジェネティクス解析が急速に進むことが考えられる。

おわりに

ハイスループットな解析手法の出現によって小児悪性固形腫瘍の基礎研究においても，各腫瘍に特異的な病因遺伝子や予後関連遺伝子等の未知の遺伝子を効率よく検索することができると考えられ，肝芽腫における早急な遺伝子検索が待たれる。

文　献

1) Ikeda H, Matsuyama S, Tanimura M：Association between hepatoblastoma and very low birth weight：a trend or a chance? J Pediatr **130**：557-560, 1997
2) Hughes LJ, Michels VV：Risk of hepatoblastoma in familial adenomatous polyposis. Am J Med Genet **43**：1023-1025, 1992
3) DeBaun MR, Tucker MA：Risk of cancer during the first four years of life in children from The Beckwith-Wiedemann Syndrome Registry. J Pediatr **132**：398-400, 1998
4) Tomlinson GE, Douglass EC, Pollock BH, et al：Cytogenetic evaluation of a large series of hepatoblastomas：numerical abnormalities with recurring aberrations involving 1q12-q21. Genes Chromosomes Cancer **44**：177-184, 2005
5) Albrecht S, von Schweinitz D, Waha A, et al：Loss of maternal alleles on chromosome arm 11p in hepatoblastoma. Cancer Res **54**：5041-5044, 1994
6) Takayasu H, Horie H, Hiyama E, et al：Frequent deletions and mutations of the beta-catenin gene are associated with overexpression of cyclin D1 and fibronectin and poorly differentiated histology in childhood hepatoblastoma. Clin Cancer Res **7**：901-908, 2001
7) Zatkova A, Rouillard JM, Hartmann W, et al：Amplification and overexpression of the IGF2 regulator PLAG1 in hepatoblastoma. Genes Chromosomes Cancer **39**：126-137, 2004
8) Sugawara W, Haruta M, Sasaki F, et al：Promoter hypermethylation of the RASSF1A gene

predicts the poor outcome of patients with hepatoblastoma. Pediatr Blood Cancer 49 : 240-249, 2007
9) Fukuzawa R, Umezawa A, Ochi K, et al : High frequency of inactivation of the imprinted H19 gene in "sporadic" hepatoblastoma. Int J Cancer 82 : 490-497, 1999
10) Nagata T, Takahashi Y, Ishii Y, et al : Transcriptional profiling in hepatoblastomas using high-density oligonucleotide DNA array. Cancer Genet Cytogenet 145 : 152-160, 2003
11) Yamamoto G, Nannya Y, Kato M, et al : Highly sensitive method for genomewide detection of allelic composition in nonpaired, primary tumor specimens by use of affymetrix single-nucleotide-polymorphism genotyping microarrays. Am J Hum Genet 81 : 114-126, 2007
12) Nannya Y, Sanada M, Nakazaki K, et al : A robust algorithm for copy number detection using high-density oligonucleotide single nucleotide polymorphism genotyping arrays. Cancer Res 65 : 6071-6079, 2005
13) Zhao X, Li C, Paez JG, et al : An integrated view of copy number and allelic alterations in the cancer genome using single nucleotide polymorphism arrays. Cancer Res 64 : 3060-3071, 2004

Molecular Biology of Hepatoblastomas

MAKOTO SUZUKI[*1], HITOSHI IKEDA[*1], SEISHI OGAWA[*2], YASUHIDE HAYASHI[*3]

*[1]*Department of Pediatric Surgery, Koshigaya Hospital, Dokkyo Medical School*
*[2]*The 21st Century COE program, Graduate School of Medicine, University of Tokyo*
*[3]*Department of Hematology and Oncology, Gunma Children's Medical Center*

Key words : Hepatoblastoma, Microarray, LOH, Methylation.
Jpn. J. Pediatr. Surg., 39(11) ; 1364～1368, 2007.

Conventional cytogenetic analyses of the chromosomal aberrations in HBL that were performed using standard karyotyping, fluorescence in situ hybridization (FISH), and comparative genomic hybridization (CGH) have been reported. Although these analyses have identified several chromosomal aberrations, the tumor-associated genes of HBL are yet to be identified. In recent years, a high-resolution genomic approach has been used to screen for genomic alterations systematically. The availability of microarray-based high-density analysis allows a reproducible and rapid determination of genome-wide alterations, and the pathogenesis of HBL should be revealed in the near future as a result.

* * *

Drash 症候群の 2 例

群馬県立小児医療センター　内科，*総合太田病院　小児血液腫瘍科（現所属）
設楽利二*　丸山健一

群馬県立小児医療センター　外科
鈴木則夫

群馬大学　小児科
小川哲史

獨協医大越谷病院　小児外科
池田　均

はじめに

Wilms 腫瘍，男性仮性半陰陽，腎症を合併するものは，1970年の Drash らの報告以来 Drash 症候群（Denys-Drash 症候群）と呼ばれている[1]．Wilms 腫瘍または男性仮性半陰陽のいずれか一つを合併した腎症もその予後は悪く，これらは広義の Drash 症候群または incomplete type Drash syndrome とされている．今回我々は Wilms 腫瘍に腎症を合併した Drash 症候群の 2 例を経験したので報告する．

症　例

症例 1：発症時 6 歳 4 カ月，女児．発症時の経過[2]は既に報告しているので腎不全の経過のみ示す．発症時に血尿を認めたが，尿蛋白は陰性であった．外表奇形や外性器の異常はみられなかった．右腎摘出術施行し Wilms 腫瘍，Stage I と診断される．日本ウィルムス腫瘍研究グループ（JWiTS），EE-4A による治療を開始．治療開始 1 年 2 ヵ月後，両側肺転移が出現．再発治療終了後の 8 歳時に蛋白尿（3＋）出現．腎機能はこの時点では大きな異常は見られなかったが，その後腎機能が進行性に悪化した（図 1）．約 5 年後の13歳時に腎機能低下が高度となったため腎移植目的で清瀬小児病院に転院となった．血中 BUN，Cr がそれぞれ292mg/dl，23.9mg/dl となった時点で血液透析を開始した．血液透析・腹膜透析継続の後，14歳 1 カ月時に母親からの腎移植を施行した．再発後現在まで 7 年 1 カ月再再発の所見無く良好である．遺伝子解析にて WT 1 遺伝子の変異が認められたことから臨床所見とあわせ Drash 症候群と診断した．

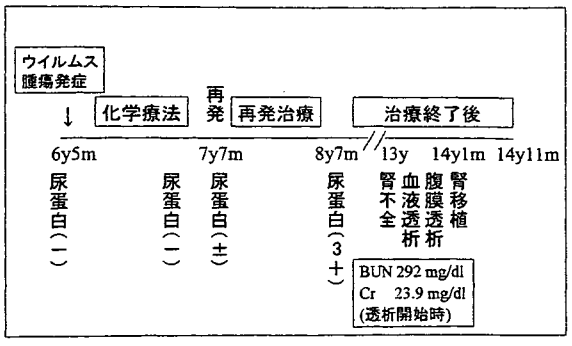

図 1　臨床経過（症例 1）

症例 2：発症時 1 歳 5 ヵ月，女児．腹部腫瘤に気付かれ，群馬大学小児科入院．腹部所見

にて右腹部に腫瘤を触知した．外表奇形や外性器の異常はみられなかった．CTにて右腎腫瘍が確認され左腎の病変も疑われた．右腫瘍腎尿管合併摘除，左腎部分（楔状）切除，腫瘍核出を施行．左腎の切除断端に腫瘍遺残を認めた．手術所見より両側性 Wilms 腫瘍，stage-V, nephroblastic type, focal nephroblastic subtype と診断．術後は National Wilms Tumor Study (NWTS)-3 の治療プロトコールに従い化学療法と腹部照射16Gy を施行．その後は再発無く経過し off therapy となった（図2）．一方，初診時より中等度の蛋白尿が認められていたが，原因は明らかではなかった．5歳時，蛋白尿の精査を目的に再入院し左腎開放生検を施行．30%の糸球体に global または segmental sclerosis を認め，巣状糸球体硬化症と診断した（図3）．蛍光抗体法では免疫グロブリン，補体の沈着は見られなかった．その他の検査成績では低蛋白血症と軽度腎機能障害が認められた（表1）．生検所見および臨床経過から Drash 症候群と診断した．その後腎機能低下が進行したが，10歳時には拡張型心筋症を発症したため腎移植も適応とはならなかった．11歳で腎不全に至り腹膜透析を開始するも13歳で腎不全および心不全にて死亡した．

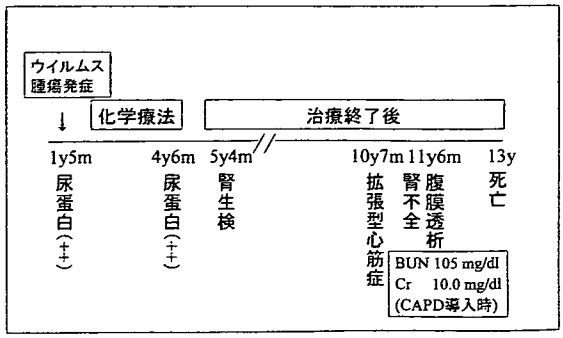

図2　臨床経過（症例2）

図3　腎生検所見（症例2）
30%の糸球体に global または segmental sclerosis を認め，巣状糸球体硬化症と診断．

考　　案

Wilms 腫瘍に腎疾患，生殖器奇形を合併したものを Drash 症候群（Denys-Drash 症候

表1　検査成績（症例2）

Ht	35.9%	Na	139mEq/l
Hb	11.4g/dl	K	4.3mEq/l
RBC	435×10⁴/cmm	Cl	1.3mEq/l
WBC	10,000/cmm	Ca	9.2mg/dl
Pl	41×10⁴/cmm	P	4.6mg/dl
		β_2-MG	2.14mg/l
T-P	5.6g/dl		
Alb	3.3g/dl	染色体	46XX
GOT	25IU/l		
GPT	9IU/l	検尿	
LDH	458IU/l	蛋白（＋＋＋）	295mg/dl
ALP	540IU/l	潜血（−），糖（−）	
		尿中 NAG	6.6U/l
BUN	28mg/dl	尿中 β_2-MG	0.58mg/l
Cr	0.9mg/dl		
T-cho	233mg/dl	＊遺伝子解析未施行	

群）という．今回報告した症例のうち症例1はWilms腫瘍発症当初は尿蛋白陰性であり，途中から蛋白尿を認めた症例である．Drash症候群における腎症が通常は症例2のように乳児期より始まる蛋白尿であることを考えると，Drash症候群の発症も様々であると思われる．またWilms腫瘍の発生頻度は低いが，進行性の腎障害と性分化異常を特徴とする疾患をFrasier症候群[3]といい，Drash症候群との異同が近年話題となっている（表2）．

Drash症候群にWilms腫瘍を発症した症例では治療後に腎不全を発症するリスクが高い[4]．

最近のNWTSでの分析ではWilms腫瘍における治療後の腎不全の発症は両側性Wilms腫瘍およびDrash症候群が危険因子としてあげられている[4]．今回の報告の症例はWilms腫瘍治療後の腎障害として発症した症例であるが，症例1ではWT1遺伝子変異を有しており，また症例2は両側性のWilms腫瘍に発症時から蛋白尿を認めていた．したがって両症例とも腎不全発症の先天的要因を持ち合わせていた可能性がある．NWTSの報告[4]ではWilms腫瘍片側例で診断後20年を経過して透析や腎移植を必要とする症例はDrash症候群で74%，WAGR症候群で36%，泌尿生殖器奇形をともなう症例で6.7%であるのに対し，これらの危険因子を持たない症例では0.6%のみと報告され，先天異常と腎障害の関係を指摘している（図4）．また同報告[4]によればWilms腫瘍両側例の

表2　Frasier症候群とDenys-Drash症候群の比較

	Frasier症候群	Denys-Drash症候群
表現型	女性	男性
性腺	streak gonad （索状性腺）	ambiguous gonad pseudohermaphroditism
病因	WT1のKTS+/−比の変化	WT1 zinc finger蛋白の変異 dominant negative
遺伝子変異	exon 9のsplice site donor mutation	*Wt*1 exon 5-9の missense mutation
腎の変化	思春期以降腎不全に至る巣状糸球体硬化症	先天ネフローゼ DMS
腫瘍	donad blastoma （性腺芽腫）	Wilms腫瘍

香坂ら[3]より，一部改変

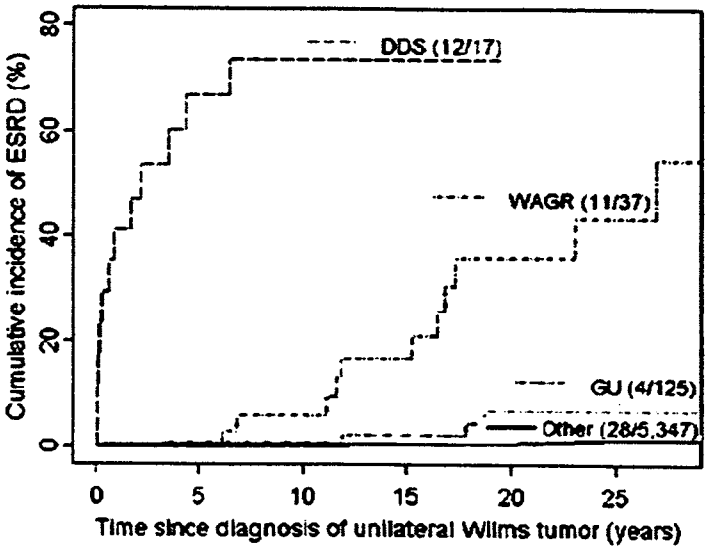

図4　片側症例治療後の腎障害
Cumulative incidence of end stage renal disease (*ESRD*) reported for patients with unilateral Wilms tumor. *DDs*, Denys-Drash syndrome. *GU*, genitourinary. *WAGR*, Wilms tumor-aniridia.

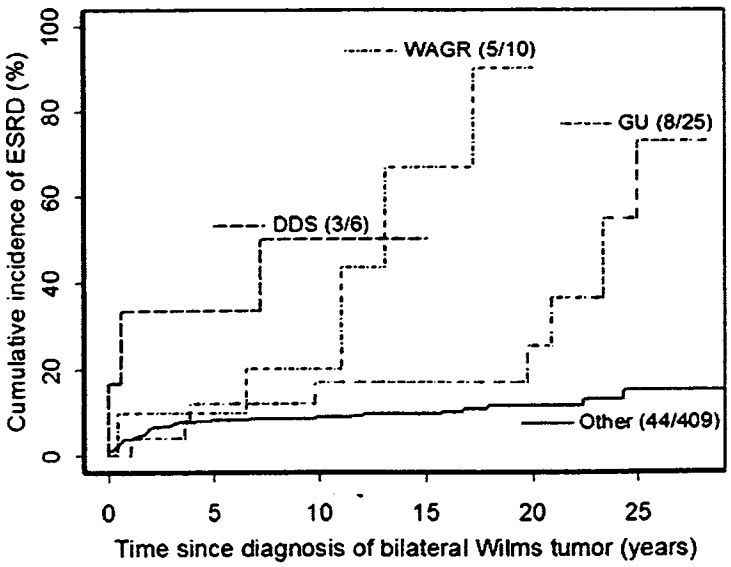

図5　両側症例治療後の腎障害
Cumulative incidence of end stage renal disease (*ESRD*) reporoed for patients with bilateral Wilms tumor. *DDS*, Denys-Drash syndrome. *GU*, genitourinary. *WAGR*, Wilms tumor-andridia.

診断後20年を経過して透析あるいは腎移植を必要とする症例はDrash症候群で50%，WAGR症候群で90%，泌尿生殖器奇形をともなう症例で25%であるが，それ以外の症例でも12%の頻度であると報告されており，両側例治療後の腎障害の頻度が高いことを指摘している（図5）．

本症候群及びその腎症の成因は不明であるが，WT 1遺伝子異常に伴う先天性の要因，すなわち腎と生殖器との分化が起る以前の胎芽期における共通の異常によって発症するものと推測されている．今後はこれらの腎不全の危険因子を持つ症例をスクリーニングし発症早期より対策を講じることが望まれる．

ま と め

Wilms腫瘍治療後に腎不全を来したDrash症候群の2例を報告した．1例は母親からの腎移植を行い，その後再発もなく現在まで経過良好であるが，他の1例は心筋症を合併し死亡した．Drash症候群はWilms腫瘍における治療後の腎不全発症の危険因子として両側性Wilms腫瘍とともにあげられている．腎不全の危険因子を持つ症例の早期の把握が望まれる．

稿を終えるにあたり，症例1の腎移植を含む診療を行って頂いた，清瀬小児病院 腎内科・内分泌代謝科その他の諸先生方に深謝致します．

文　献

1）Drash A, Shermann F, Hartmann WH, et al : A syndrome of pseudohermaphroditism, Wilms' tumor, hypertension, and degenerative renal disease. J Pediatr 76 (4) : 585-93, 1970

2）設楽利二，清水宏之，嶋田　明，他：肺転移をきたしたstage-I Wilms腫瘍の一例における診断上の問題点の検討．小児がん 41 (4)：870-874，2004

3）香坂隆夫，田川　学，肥沼正夫，他：Frasier症候群．日本臨床 June 28 ; Supple 2 : 499-504, 2006

4）Breslow NE, Collins AJ, Ritchey ML, et al : End stage renal disease in patients with Wilms tumor : Results from the National Wilms Tumor Study Group and the United States Renal Data System. J Urol 174 : 1972-1975, 2005

Whole-genome profiling of chromosomal aberrations in hepatoblastoma using high-density single-nucleotide polymorphism genotyping microarrays

Makoto Suzuki,[1,6] Motohiro Kato,[2] Chen Yuyan,[2] Junko Takita,[3] Masashi Sanada,[4] Yasuhito Nannya,[4] Go Yamamoto,[4] Atsushi Takahashi,[1] Hitoshi Ikeda,[6] Hiroyuki Kuwano,[1] Seishi Ogawa[5,8] and Yasuhide Hayashi[7,8]

[1]Department of General Surgical Science, Graduate School of Medicine, Gunma University Graduate School, 3-39-15 Showa, Maebashi, Gunma 371-8511; [2]Department of Pediatrics, [3]Department of Cell Therapy and Transplantation Medicine, [4]Department of Hematology and Oncology, and [5]The 21st century COE program, Graduate School of Medicine, University of Tokyo, 7-3-1 Hongo, Bunkyo-ku, Tokyo 113-8655; [6]Department of Pediatric Surgery, Koshigaya Hospital, Dokkyo Medical School, 2-1-50 Minami-Koshigaya, Koshigaya, Saitama 343-8555; [7]Department of Hematology and Oncology, Gunma Children's Medical Center, 779 Shimohakoda, Hokkitsu, Shibukawa, Gunma 377-8577, Japan

(Received July 31, 2007/Revised November 14, 2007/Accepted November 17, 2007/Online publication January 2, 2008)

To identify the genomic profile and elucidate the pathogenesis of hepatoblastoma (HBL), the most common pediatric hepatic tumor, we performed high-density genome-wide single-nucleotide polymorphism (SNP) microarray analyses of 17 HBL samples. The copy number analyzer for GeneChip® (CNAG) and allele-specific copy number analysis using anonymous references (AsCNAR) algorithms enabled simple but sensitive inference of allelic composition without using paired normal DNA. Chromosomal aberrations were observed in 15 cases (88%). Gains in chromosomes 1q, 2 (or 2q), 8, 17q, and 20 and losses in chromosomes 4q and 11q were frequently identified. High-grade amplifications were detected at 7q34, 14q11.2, and 11q22.2. Several types of deletions, except homozygous deletion, were identified. Most importantly, copy-neutral loss of heterozygosity (uniparental disomy [UPD]) at 11p15 was detected in four of the 17 HBL samples. Insulin-like growth factor II (*IGF2*) and *H19* genes were located within this region. The methylated status of this region indicated the paternal origin of the UPD. The expression patterns of *IGF2* and *H19* were opposite between genes with and without the UPD. This difference in the expression patterns might influence the clinical features of HBL. (*Cancer Sci* 2008; 99: 564–570)

Hepatoblastoma (HBL) is the most common pediatric hepatic tumor predominantly observed in infants and children aged less than 3 years.[1–3] The dramatic increase in the survival of patients that has been observed during the last three decades is mainly due to advances in the use of chemotherapy and surgical techniques.[1–3] Currently, approximately 75% of children with HBL can be cured completely, although a large tumor, a multifocal tumor, and metastatic spread are all associated with a fatal outcome.[3] The etiology of HBL remains unknown. Most HBL are sporadic; however, an association with prematurity or low birth weight,[4] and genetic disorders such as familial adenomatous polyposis (FAP),[5] or Beckwith–Wiedemann syndrome (BWS) has been documented.[6] These findings imply that an alteration at 11p15, which is the critical region in BWS and critical to the wingless signaling pathway involving the adenomatosis polyposis coli (*APC*) gene that is constitutionally mutated in FAP patients,[7,8] could also play a role in the genesis of sporadic HBL. Indeed, the loss of heterozygosity (LOH) at 11p15 and mutations in the *APC* and β-catenin genes have also observed in some sporadic HBL.[9,10]

LOH and deletion of tumor suppressor genes are observed frequently in malignant cells and can be associated with the deregulation of cell fate and apoptosis.[11] Similarly, amplification of the chromosomal regions can increase the expression of oncogenes during tumor progression. Conventional cytogenetic analyses of chromosomal aberrations in HBL performed using standard karyotyping,[12–16] fluorescence *in situ* hybridization (FISH),[17–20] and comparative genomic hybridization (CGH),[21,22] have been reported. Although these analyses have identified several chromosomal aberrations in HBL, predominantly the gains in chromosomes 1q, 2, 8q, 17q, and 20 and the loss in chromosome 4q, the tumor-associated genes of HBL involved in these genomic copy number (CN) alterations are yet to be identified.

In recent years, a high-resolution genomic approach has been used for the systematic screening of chromosomal CN alterations. The availability of microarray-based high-density single-nucleotide polymorphism (SNP) analysis allows a reproducible and rapid determination of genome-wide alterations.[23–25] The Affymetrix® GeneChip® platform, originally developed for large-scale SNP typing, has a unique feature compared with array-based CGH: it enables the genome-wide detection of LOH in addition to extremely high-resolution CN analysis of cancer genomes by using large numbers of SNP-specific probes. The density, distribution, and allele specificity of SNP render them an excellent candidate for the high-resolution analyses of LOH and CN alterations in cancer genomes.[26,27] Conventionally, LOH analyses require the comparison of the genotypes of the tumor and its normal germline counterpart. However, for the analysis of cell line, xenograft, leukemia, and archival samples, paired normal DNA is often unavailable. In the absence of a paired normal DNA sample, LOH is inferred only based on the lower-than-expected frequencies of heterozygous SNP calls in the tumor samples. However, the low tumor content within the samples greatly hampers the sensitive detection of LOH due to increased heterozygous SNP calls. To overcome these difficulties with the current algorithms, we have recently developed novel algorithms (copy number analyzer for GeneChip® [CNAG] and allele-specific copy number analysis using anonymous references [AsCNAR]) to analyze the allelic composition of cancer genomes based on the microarray data obtained from the GeneChip® platform.[27,28] These algorithms calculate the allele-specific CN independent of the availability of a paired control DNA, enabling the sensitive detection of both LOH and CN alterations in a wide spectrum of primary tumor specimens. The performance of the new algorithm was demonstrated by detecting the neutral CN LOH or uniparental disomy (UPD) in a large number of acute leukemia samples.[28]

[8]To whom correspondence should be addressed.
E-mail: hayashiy-tky@umin.ac.jp; sogawa-tky@umin.ac.jp

doi: 10.1111/j.1349-7006.2007.00710.x

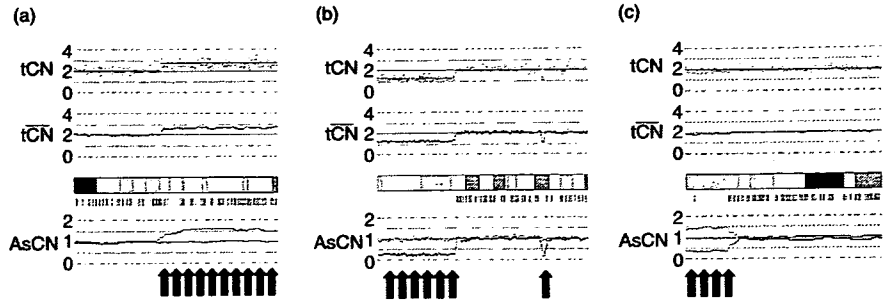

Fig. 1. Representative results of the allele-specific copy number analysis using anonymous references (AsCNAR) program with regard to copy number (CN) alterations detected in our series at particular loci, such as (a) gain (b) chromosomal loss, and (c) uniparental disomy (UPD), which have not been detected using conventional algorithms. The red dots indicate the raw CN plot for each single-nucleotide polymorphism (SNP), and the blue lines indicate the local mean CN of five SNP. The vertical green bar indicates the heterozygous SNP calls.

In the present study, to identify the novel genomic alterations in sporadic HBL cases, we performed high-resolution analyses of genome-wide CN alterations such as gains, losses, allelic imbalances, and amplifications of small chromosomal regions. Due to the high resolution of the SNP arrays and the new algorithm AsCNAR, we could systematically identify several amplifications, deletions, and allelic imbalances, including the UPD.

Materials and Methods

Patients and samples. We obtained 17 primary HBL samples at the time of diagnosis from five patients treated at the Gunma Children's Medical Center and 12 patients treated at different institutes in Japan, including Saitama Children's Medical Center. No patient had received chemo- and/or radiotherapy before the biopsy of the primary tumors. After obtaining informed consent from the parents and approval for the study from the institutional review board of each institute, all the HBL samples were subjected to genomic DNA extraction using the QIAamp DNA Mini Kit (Qiagen, Chatsworth, CA, USA) according to the manufacturer's instructions. Total RNA was extracted from the frozen stocked tumors using the Isogen reagent (Nippon Gene, Osaka, Japan), according to the manufacturer's instructions. The total RNA was reverse transcribed to synthesize cDNA using the Ready-To-Go T-Primed First-Strand Kit (GE Healthcare Bio-Sciences, Piscataway, NJ, USA).

SNP array analysis. The array experiments were performed according to the standard protocol of Affymetrix® GeneChip® Mapping 50K *Xba*I Array (Affymetrix, Inc., Santa Clara, CA, USA). In brief, the total genomic DNA (250 ng from each sample) was first digested with a restriction enzyme (*Xba*I). The digested DNA was then ligated to an appropriate adapter that recognized the four cohesive base pair (bp) overhangs, and polymerase chain reaction (PCR) amplification was performed using a single primer that recognized the adapter sequence. After fragmentation with DNase I, the PCR products were labeled with a biotinylated nucleotide analog using terminal deoxynucleotidyl transferase, and the labeled products were hybridized to the GeneChip® Human Mapping 50K Array for 17 h. Subsequently, the arrays were washed, stained, and scanned.

The genotype calls and the intensity of the SNP probes were determined using GeneChip Operation software (GCOS; Affymetrix, Inc.). The SNP CN and chromosomal regions with gains or losses were individually evaluated using the CNAG[27] and AsCNAR algorithms,[28] which enabled an accurate determination of allele-specific CN as well as the sensitive detection of LOH even in the presence of normal cell contamination of up to 70–80% without requiring constitutive DNA (Fig. 1; http://www.genome.umin.jp).

Validation of CN alterations using the interphase FISH. We performed FISH to validate the CN status obtained using the SNP array analysis. FISH probes were prepared using the BAC clones RP11-185M22, RP11-80P10, and RP11-86M15. Each BAC DNA was purified, and 100 ng of the clone was labeled with digoxigenin-dUTP using random primers; these labeled clones were used as probes for FISH analysis by following the established protocols.[29,30]

Quantitative real-time PCR and reverse transcription (RT)-PCR. Real-time quantitative PCR (RQ-PCR) and real-time quantitative RT-PCR (RQ-RT-PCR) analyses were carried out to quantify the relative CN of several amplifications in the HBL samples and the expression levels of the defender against cell death 1 (*DAD1*), EPH receptor B6 (*EphB6*), *ErbB4*, insulin-like growth factor II (*IGF2*), and *H19* genes using a Power SYBR Green PCR Master Mix (Applied Biosystems, Foster City, CA, USA) with an ABI prism 7700 real-time PCR detection system (Applied Biosystems). The primer pairs were designed using PrimerExpress software (Applied Biosystems) and synthesized by Invitrogen (Carlsbad, CA, USA).The primer sets used for the RQ-PCR experiments are listed in Table 1. Data were captured using Sequence Detection

Table 1. Primers used for polymerase chain reaction (PCR) analyses

Gene	Primer forward	Primer reverse
(Genomic RQ-PCR)		
EphB6	GGACTGCAACTGAACGTCAA	TCTGGAAAGGAAGCAAAGGA
DAD1	GTTATGTCGGCGTCGGTAGT	GTCCCCACGAGGAGACAGTA
(RQ-RT-PCR)		
ERBB4	AACAGCAGTACCGAGCCTTG	CCAGAGGCAGGTAACGAAAC
DAD1	CGAGCCTTTGCTGATTTTCT	TCCAATAAGCTGCCATCTCC
IGF2	CTCTCCGTGCTGTTCTCTCC	TATCGGGAAATGAGGTCAGC
H19	GAAGGAGGTTTAGGGGATCG	TTGCTCTTTCTGCCTGGAAC
(Bisulfite PCR/RQ-PCR)		
H19DMR (Methylated)	GGTACGGTTTTTTTAGGTTTATGTC	ACCCCTACAACCTCCTTACTACG
H19DMR (Unmethylated)	TATGGTTTTTTTAGGTTTATGTTGG	ACCCCTACAACCTCCTTACTACAC

Primers and probes were designed using Primer Express software and MethPrimer software. RQ-PCR, real-time quantitative PCR; RQ-RT-PCR, real-time quantitative reverse transcription-PCR.

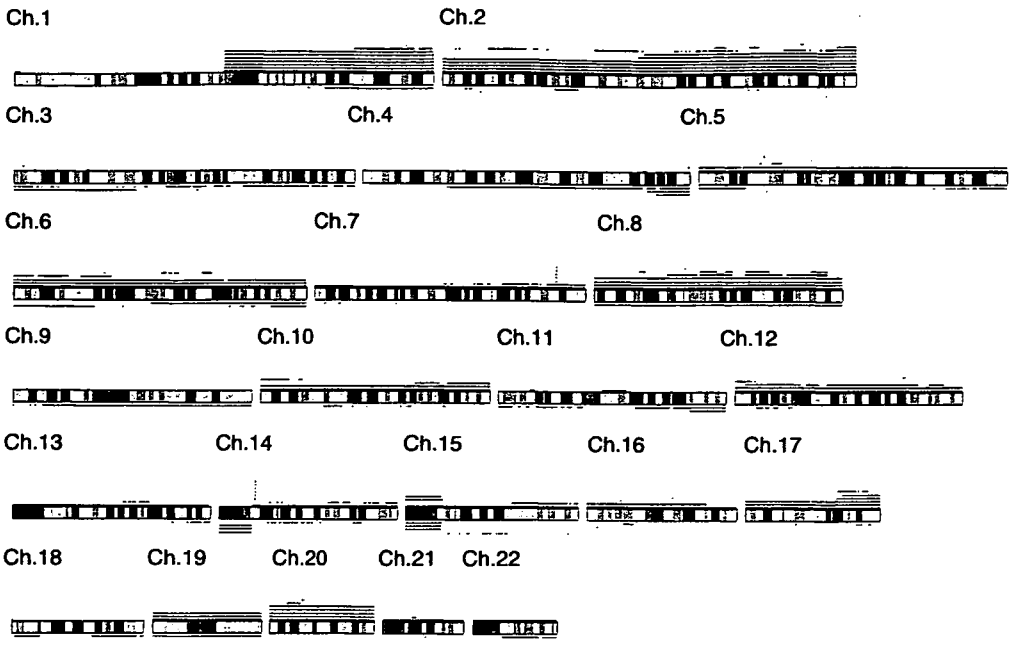

Fig. 2. Overview of the DNA copy number (CN) gains and losses detected in 17 hepatoblastoma (HBL) samples. A gain is indicated by the red bar above the chromosome ideogram, and a loss is indicated by the green bar under the chromosome ideogram. Each horizontal line represents an aberration detected in a single tumor.

software (version 1.7a; Applied Biosystems). For each primer pair, a standard curve was generated from five-fold serial dilution from approximately 50–80 pg of control DNA from a healthy individual. The amounts of genomic DNA and cDNA used in each test and the reference marker for all HBL samples were calculated using the appropriate standard curve. Normalization was performed using the β-actin gene as the internal control.

Sodium bisulfite modification and methylation-specific PCR. The genomic DNA from the tumor samples was treated with sodium bisulfite as described previously.[31] Briefly, 1 μg of DNA was denatured with sodium hydroxide and modified with sodium bisulfite. The modified DNA was then purified with the Wizard® DNA Clean-Up System (Promega, Madison, WI, USA), precipitated with ethanol, resuspended in Tris-EDTA (TE) buffer (pH 8.0), and either used immediately or stored at –20°C until use. The bisulfite-modified DNA was amplified with primer pairs for the methylated and unmethylated complete sequences upstream of the *H19* promoter CpG islands in the HBL samples with UPD in 11p15. The primer pairs were designed using MethPrimer software,[32] and synthesized by Invitrogen. The primers for methylation-specific DNA and unmethylation-specific primers are listed in Table 1. Normal lymphocyte DNA was used as the control. PCR was carried out in a 25 μL reaction volume using Ex Taq Hot Start Version (TaKaRa Bio Inc., Kyoto, Japan). The PCR conditions were as follows: 1 cycle at 95°C for 10 min; followed by 35 cycles of 94°C for 30 s, 60°C for 30 s, 72°C for 2 min; and a final extension at 72°C for 5 min. The PCR products were separated on 3% agarose gels and visualized under UV illumination after ethidium bromide staining. To quantify the ratio of the methylation status, we also carried out the methylation-specific RQ-PCR analysis.

Results

Detection of CN alterations in HBL samples. We investigated 17 HBL samples obtained from the sporadic cases of HBL by using the Affymetrix® GeneChip® 50K *Xba*I Mapping Array. Although these specimens did not contain paired control DNA and had varying degrees of normal tissue contamination, the genomic alterations were accurately determined in most specimens by our CNAG/AsCNAR program (Fig. 1). The real CN and LOH status was inferred from the observed signal ratios of the tumor to the reference, based on the hidden Markov models implemented in the CNAG/AsCNAR program; these are summarized in Fig. 2. The CN data were validated at a number of SNP sites using FISH analysis of the cell nuclei extracted from the HBL samples (Fig. 3). The CN data obtained using the FISH analyses were consistent with those obtained using SNP mapping.

Numerical chromosomal aberrations were observed in 15 HBL samples (88%), excluding two HBL samples (HBL_22 and HBL_250). These 15 cases had variable degrees of CN gains and losses; however, the gains including the amplifications were more frequent than the losses (Table 2 and Fig. 2). Total or partial gains in chromosomes 1q and 2 were the most frequent aberrations detected in eight of the 17 patients (47%). The gain in chromosome 8 was the second most frequent aberration detected in five of the 17 samples (29%). The gains in chromosomes 17q and 20 were observed in 24% of the cases (four of 17 cases). The LOH in chromosomes 4q and 11q was observed in three (18%) and two (12%) of the 17 samples, respectively. However, these regions were usually large, and we could not determine the presence or absence of alterations in specific genes within these regions.

High-grade amplification and common deletion. High-grade amplifications are of particular interest because they may indicate the loci of oncogenes. The regions with high-grade amplification were defined as segments with at least five SNP loci with an inferred CN of >5. High-grade amplifications of 7q34 and 14q11.2 were observed in five (29%) and nine (53%) HBL samples, respectively. For the validation of the amplifications observed using the SNP array, FISH analysis and genomic RQ-PCR were performed. To determine the genes that are potentially affected at 14q11.2, several genes localized at the 14q11.2 chromosomal region with overlap or proximity to the BAC-RP11-85M16 were examined using the UCSC browser (www.genome.ucsc.edu). Genes that map to these regions include *EphB6* and *DAD1*, which are identified as the negative regulators of apoptosis. These two genes were subjected to RQ-PCR. FISH analysis with RP11-85M16 BAC clone probe showed multiple signals, confirming

doi: 10.1111/j.1349-7006.2007.00710.x

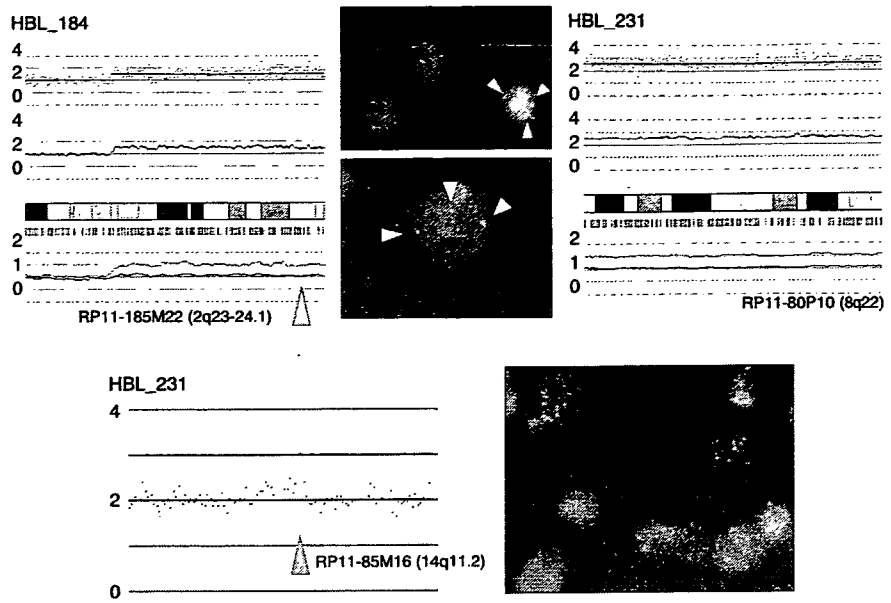

Fig. 3. Representative results of array analysis of hepatoblastoma (HBL) samples (HBL_184 and HBL_231). Fluorescent *in situ* hybridization analysis with BAC probes confirmed the detected changes. We detected three signals from chromosomes 2q and 8q. At the high-amplification region of chromosome 14q, three and more signals were detected.

Table 2. Chromosomal aberrations in 17 primary hepatoblastoma (HBL) samples

Sample	Copy number gain	Copy number loss	Uniparental disomy
HBL_4	1q, 2q34, 5p13.1, 17q23.3-qter	3p13-pter, 3q13.11, 6q14.1-qter, 11q23.1-qter	Not detected
HBL_7	1q, 2, 8, 14q11.2, 20	not detected	11p15.4-pter
HBL_8	7q34	not detected	Not detected
HBL_9	1q, 2q14.1-qter, 6p, 7, 14q11.2	6p12.1, 9p21.1	Not detected
HBL_12	8q11.23, 10q21.3, 10q26.13, 14q11.2, 22q13.31	7q35	Not detected
HBL_14	2p16.3-p22.3, 2p23.1, 2q11.2-q14.1, 2q33.1-q34, 3p21.33-p22.1, 3p24.2, 3p25.1, 3p25.2, 4q32.2-q32.3, 5p13.2, 6q14.3-q16.1, 7q, 11p15.1, 10p13-pter, 11q22.2-q22.3, 12p13.2-pter, 14q23.3-q31.1, 15q22.31-q26.2, 16p12.3, 20p11.23	1q31.1-qter, 2p12-14, 3, 4q, 5p14.1-pter, 5q32-qter, 6p12.13-pter, 6q11.1, 6q25.1-qter, 8, 9, 12p11.1-13.1, 17q24.3, 18p11.21-11.32, 18q21.1-qter, 19, 22	Not detected
HBL_22	Not detected	Not detected	Not detected
HBL_27	1q, 2q24.2-24.3, 7q34, 14q11.2	4q32.3-qter, 16p12.1	Not detected
HBL_28	3p26.1, 7q34, 14q11.2, 20	2p24.1	11p14.3-pter
HBL_34	1q, 2, 7q34, 14q11.2, 17	4q34.1-qter	Not detected
HBL_36	1q32.1-qter	1p13.3-pter, 4q21.22-qter, 5p13.1	Not detected
HBL_37	1q, 2, 5, 6, 7q34, 8, 10, 12, 14, 14q11.2, 15, 16q22.1-pter, 17, 19, 20	Not detected	11p15.2-pter, 16q22.2-qter
HBL_184	2q14.2-qter, 3p24.3, 4q33, 10p14, 11p14.3, 14q11.2	Not detected	Not detected
HBL_185	6p, 21q21.2	Not detected	Not detected
HBL_231	8, 14q11.2, 19, 20	Not detected	11p15.4-pter
HBL_246	1q, 2, 5, 6, 8, 10, 12, 13, 16, 17, 19, 20, 21, 22	Not detected	4, 9
HBL_250	Not detected	Not detected	Not detected

CN gains at 14q11.2 (Fig. 3). Further, in RQ-PCR analysis, the CN gain of *EphB6* and *DAD1* was evident in all samples that showed high-grade amplification in SNP array (data not shown). Other high-grade amplifications are listed in Table 3. The size of these amplicons was typically less than 1 Mb, and the possible genes present in these regions are summarized in the same table. All these candidate genes, except *MMP7*, have not been reported previously with regard to HBL.[33]

Homozygous deletions are also of particular interest because they may indicate a tumor suppressor gene. However, homozygous deletions were not identified in any sample.

CN neutral LOH (UPD). LOH can be more sensitively detected with the CNAG/AsCNAR algorithms by evaluating the allele-specific CN than from the grossly reduced heterozygous SNP calls, particularly when the SNP shows no CN losses. The UPD regions were identified in five of the 17 samples. In four samples (HBL_7, HBL_28, HBL_37, and HBL_231), 11p15 was the common UPD region (Fig. 4a). Other UPD regions were observed within chromosomes 4, 9, and 16q22 (Table 2). The candidate target genes that map to the UPD region located within 11p15 include *IGF2* and *H19*. Methylation-specific PCR analysis was performed for the four HBL samples having UPD within 11p15 to identify the origin of the amplified allele. The methylation status of the differential methylated region (DMR) of *H19* is shown in Fig. 4b. Hypermethylation of the *H19* DMR was detected in all HBL samples having UPD within 11p15; however, normal lymphocyte DNA showed the mosaic methylation pattern. In general, the *H19* DMR is hypermethylated on the paternal allele

Table 3. High-grade amplifications in hepatoblastoma (HBL) samples

Cytoband	Implicated region (base pairs)		Candidate target genes in the region
	Start–end	Size	
2q34	211 193 864–212 239 181	1 045 318	*ErbB4*
3p25.2	11 888 124–12 876 175	988 052	*RAF1*
7q34	141 721 559–142 076 238	354 680	*EphB6*
11q22.2-q22.3	101 394 973–102 830 195	1 435 223	*MMP1, 7, 20*
14q11.2	21 426 631–22 130 392	703 762	*DAD1*

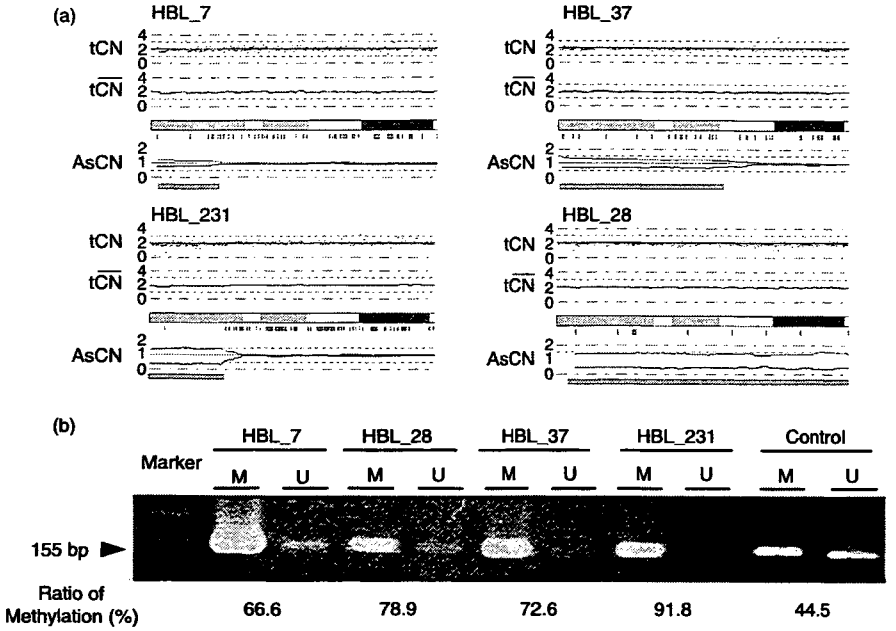

Fig. 4. (a) Copy numbers (CN) of chromosome 11p in four hepatoblastoma (HBL) samples with uniparental disomy (UPD). Although complete CN alterations are not observed, UPD is clearly predicted based on the allele-specific CN alterations (green lines). (b) Methylation-specific polymerase chain reaction (PCR) analysis of the *H19* differential methylated region (DMR). Modified DNA was amplified with primer pairs for methylated and unmethylated complete sequences of the *H19* DMR. *H19* DMR hypermethylation was detected in all HBL samples; however, normal lymphocyte DNA exhibited the mosaic methylation pattern. The results of quantitative real-time methylation-specific PCR analysis are shown below the image depicting the results of electrophoresis.

and hypomethylated on the maternally expressed allele in humans. This indicates that the UPD within this region is considered to be derived from the paternal allele. Furthermore, a low expression level of the non-methylated allele was also observed; methylation-specific RQ-PCR analysis revealed that the ratio of the methylation status ranged from 66.6% to 91.8%.

Expression analyses using RQ-RT-PCR. In order to examine the impact of the abovementioned amplifications and UPD on gene expression, we measured the expression levels of four genes (*DAD1*, *ErbB4*, *IGF2*, and *H19*) through RQ-RT-PCR (Fig. 5). Normal liver total RNA served as the non-neoplastic reference and control. HBL_184 and HBL_231 for which RNA were available showed a high expression of the *ErbB4* gene. However, the expression of *DAD1* was down-regulated in both these samples. The *IGF2* and *H19* genes were oppositely expressed between HBL_184 and HBL_231, having UPD within 11p15.

Discussion

The present study represents the application of the SNP array technology for the genome-wide analysis of CN aberrations in HBL. Several recent studies and our previous research have demonstrated that this technology provided a unique opportunity to assess the DNA CN alterations and LOH simultaneously throughout the entire genome.[24–27,29] As shown in the present analysis, the use of high-resolution SNP arrays improved the ability to identify structural chromosomal aberrations in cancer cells and detect genes affected by these aberrations. Additionally, high-density SNP array analysis with the CN analyzer software can also

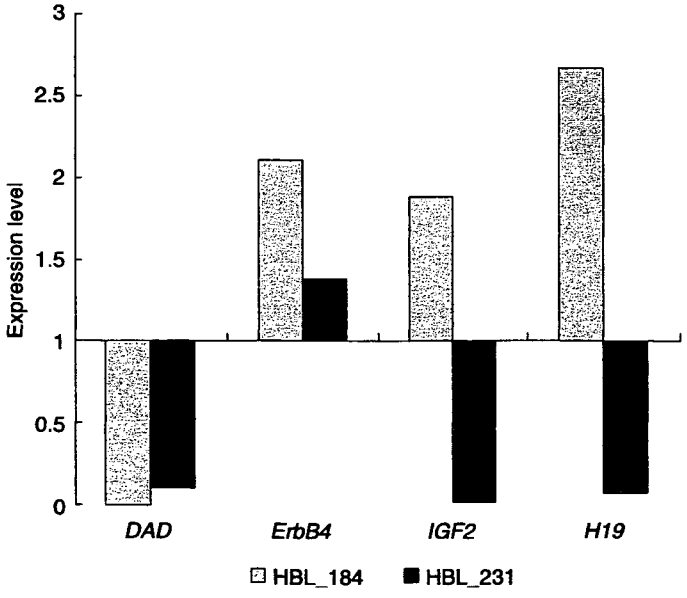

Fig. 5. The results of the expression levels of four genes (defender against cell death 1 [*DAD1*], EPH receptor B6 [*EphB6*], *ErbB4*, insulin-like growth factor II [*IGF2*], and *H19* genes) through real-time quantitative reverse transcription-polymerase chain reaction (RQ-RT-PCR) analyses.

doi: 10.1111/j.1349-7006.2007.00710.x

facilitate the identification of allelic imbalances such as copy-neutral LOH in the absence of a paired normal DNA reference.

The aberrations in chromosomes 1q, 2, 8, and 20 have been noted as the most commonly occurring aberrations in all previous reports,[21,22] as well as in the present study. In the present study, the most frequently detected aberrations were gains in chromosomes 1q and 2 (or 2q), observed in approximately 50% of the cases.

Trisomy in chromosome 1q is a well-known alteration in HBL.[34] Similar 1q imbalances have also been described in other pediatric neoplastic disorders such as lymphoma,[35] Wilms' tumor,[36] and sarcoma,[37] indicating that these aberrations are related to tumor progression. The candidate genes in 1q included the *NTRK1*, *ABL2*, *CD34*, *DAP3* (death receptor protein-3), and caspase-3 genes.[38] The anomalies in chromosome 2, which almost always result in gains in 2q, are also common in HBL. These imbalances are also commonly found in embryonal rhabdomyosarcoma and other pediatric tumors related to BWS. Translocation involving the *PAX3* gene located in 2q35 has been suggested to play a crucial role in the pathogenesis of alveolar rhabdomyosarcoma.[39] Based on this, a genetic link has been suggested between HBL and alveolar rhabdomyosarcoma. The role of the *PAX3* gene in the pathogenesis of HBL is yet to be determined. Additionally, the 2q24–32 region contains several genes that may also have an oncogenic potential. These include a serine/threonine kinase receptor, *ITRAF*, *FRZB*, a secreted antagonist of WNT signaling, and BRCA1-associated RING domain 1 (*BARD1*) genes. However, no specific gene has been identified in the previous,[21,22] and present studies.

The losses in chromosomes 4q and 11q were comprehensively observed. In hepatocellular carcinoma (HCC) cells, Wong *et al.* demonstrated a growth advantage following the loss in the 4q arm.[40] In HCC, 4q21–q22 and 4q35 have been identified as commonly deleted regions, and allelic losses in 4q35 have been associated with a larger tumor size and an aggressive histological tumor type.[41] Previous studies have not reported a significant correlation between HBL with loss in the distal 4q arm and prognosis, but the underlying oncogenic event might be due to the loss of a gene on the distal 4q arm.

Many minimal regions of amplification and deletion were detected using high-density SNP arrays, although homozygous deletion was not identified in any sample. The SNP loci located in 7q34 and 14q11.2 were found to be highly amplified in sporadic HBL samples. The candidate genes at these loci are *EphB6*, *DAD1*, and BCL-like 2 (*BCL2L2*) genes that encode the proteins associated with the execution of cell apoptosis. Gains as well as high amplifications in this region have not been reported previously; however, such an observation will be of particular interest for the discovery of oncogenes involved in the pathogenesis of HBL.

The UPD regions were identified in five of the 17 samples. This is chiefly important because UPD is being particularly considered as a possible mechanism of tumor initiation. During tumorigenesis, UPD is believed to arise due to a mitotic recombination caused by a rare crossover event during mitotic cell division. The products of mitotic recombination are the regions of the genome exhibiting UPD, and both the genomic regions originate from the same parent. We could identify a common UPD on chromosome 11p that is reminiscent of BWS with paternal UPD; in this case, the loss of function of the 11p15 maternal alleles through various mechanisms may be the critical event associated with tumorigenesis and BWS.[42] BWS is a neonatal overgrowth syndrome that predisposes an individual to cancer,[6] and the importance of the maternally active locus in chromosome 11p15 in tumorigenesis is supported by the finding that the loss of imprinted allele and paternal duplication leads to tissue overgrowth and subsequent tumor development. Methylation analysis was performed for the four HBL samples having UPD within 11p15, and hypermethylation of *H19* DMR was detected in all four HBL samples. Because *H19* DMR was hypermethylated on the paternal allele and hypomethylated on the maternally expressed allele in humans, we consider that the UPD within 11p15 was of paternal origin.

Two candidate genes, namely, *IGF2* and *H19*, are located within the telomeric region of chromosome 11p15.5 and have opposite imprinting patterns.[43] In the majority of human tissues, *IGF2* is expressed only from the paternal allele, whereas *H19* is transcribed only from the maternal allele. *H19* is an untranslated gene but has been suggested to function as a tumor suppressor.[44] In fetal and adult organs, the transcriptionally silent *H19* allele was extensively hypermethylated throughout the entire gene and its promoter. On the maternally expressed *H19* allele, *H19* DMR is unmethylated and can bind to the CTCF protein. On the paternal *H19* allele, *H19* DMR is highly methylated. This not only prevents the expression of the imprinted paternal *H19* alleles but also blocks the binding of the CTCF protein.[43] In general, the outcome of UPD with losses of the 11p15 maternal alleles in HBL is the same as that of the loss of imprinting on the inactivated, imprinted, and maternally expressed genes in BWS. Weksberg *et al.* proposed a dual pathway model for tumor development in BWS, wherein methylation defects at *H19* and/or *IGF2* in 11p15 were found to play a role in Wilms' and HBL tumorigenesis.[45] The combined loss of expressions in various 11p15-imprinted genes may contribute to tumorigenesis.

In the present study, we identified that the expression patterns of *IGF2* and *H19* were opposite between genes with and without the UPD in 11p15. This difference in the expression patterns might influence the clinical features of HBL. Further prospective studies are required to reveal any potential correlations between specific LOH and clinical outcomes.

In summary, the analysis of LOH and CN alterations using the SNP microarray in HBL samples revealed significant areas of allelic imbalance. We hypothesize that UPD, in addition to allelic imbalance, constitutes a novel genetic mechanism involved in tumorigenesis. Therefore, detailed characterizations such as functional studies should be conducted to elucidate the significance of the regions detected in this study, many of which may contain the candidate tumor suppressor genes and oncogenes involved in the pathogenesis of HBL.

Acknowledgments

This work was supported in part by a Grant-in-Aid for Cancer Research from the Ministry of Health, Labour and Welfare of Japan, a Grant-in-Aid for Scientific Research from the Ministry of Education, Culture, Sports, Science and Technology of Japan, and a grant from the 21st Century COE Program from the Ministry of Education, Culture, Sports, Science and Technology of Japan.

References

1 Roebuck DJ, Perilongo G. Hepatoblastoma: an oncological review. *Pediatr Radiol* 2006; **36**: 183–6.
2 Tiao GM, Bobey N, Allen S *et al.* The current management of hepatoblastoma: a combination of chemotherapy, conventional resection, and liver transplantation. *J Pediatr* 2005; **146**: 204–11.
3 Schnater JM, Kohler SE, Lamers WH, von Schweinitz D, Aronson DC. Where do we stand with hepatoblastoma? A review. *Cancer* 2003; **98**: 668–78.
4 Ikeda H, Matsuyama S, Tanimura M. Association between hepatoblastoma and very low birth weight: a trend or a chance? *J Pediatr* 1997; **130**: 557–60.
5 Hughes LJ, Michels VV. Risk of hepatoblastoma in familial adenomatous polyposis. *Am J Med Genet* 1992; **43**: 1023–5.
6 DeBaun MR, Tucker MA. Risk of cancer during the first four years of life in children from The Beckwith–Wiedemann Syndrome Registry. *J Pediatr* 1998; **132**: 398–400.
7 Fukuzawa R, Hata J, Hayashi Y, Ikeda H, Reeve AE. Beckwith–Wiedemann syndrome-associated hepatoblastoma: wnt signal activation occurs later in